AEGC2019 Data to Discovery
Australasian Exploration Geoscience Conference
2-5 September 2019 • Perth, Western Australia
Incorporating the AIG, ASEG, PESA, and WABS

Green's function retrieval from deterministic seismic wavefield using higher-order cross-correlation

Yunfeng Chen
Deep Earth Imaging, FSP, CSIRO
26 Dick Perry Ave, Kensington WA, 6151, Australia
yunfeng.chen@csiro.au

Erdinc Saygin
Deep Earth Imaging, FSP, CSIRO
26 Dick Perry Ave, Kensington WA, 6151, Australia
erdinc.saygin@csiro.au

SUMMARY

Seismic interferometry, commonly known as empirical Green's function retrieval in seismology, has been widely applied to extract the impulse response of Earth. The conventional approach based on cross-correlation of long-term ambient seismic wavefield relies on the simultaneous recording of noise signals at seismic receivers. Recent studies have demonstrated observationally that the correlation of coda of (ambient noise) cross-correlation function (C^3) enables the reconstruction of inter-station Green's function regardless of the operating time (i.e., synchronous or asynchronous) of stations. Here we extend the C^3 scheme to a more general framework that involves the correlation of cross-correlation function (C^2). This new approach exploits the deterministic energy of the wavefield and is more robust than C^3 that may suffer from incoherent coda wave energy due to less ideal (e.g., sparse, noisy, short duration) network configurations. We apply this technique to the recently deployed ALFREX seismic network in southwestern Australia. We show that the Green's function between asynchronous stations can be robustly recovered using the C^2 approach whereas this is not feasible from C^3. The proposed technique can effectively bridge the temporal gaps between temporary networks and demonstrate great potential for improving the spatial coverage of data and resolution in seismic imaging of crustal structures.

Key words: Seismic interferometry, deterministic wavefield, ambient noise cross-correlation, Green's function, seismic imaging, Australian crust

INTRODUCTION

The cross-correlation of the ambient seismic field has been widely applied to probe the internal structure of Earth at various scales. Both experimental (Lobkis and Weaver 2001; Weaver and Lobkis 2001) and theoretical works (see Snieder and Larose, 2013 for a review) have demonstrated that sufficient time averaging of cross-correlation of ambient wavefield (hereafter C^1) recorded at two receivers converge into inter-station Green's function (GF). Such an approach relies on the acquisition of seismic wavefield that contains diffuse energy from simultaneously acting uncorrelated sources (Wapenaar et al., 2010); this temporal constraint restricts its application to stations operating synchronously. In recent years, methods have been proposed to reconstruct the GF by cross-correlating the coda of the cross-correlation function (hereafter C^3) extracted from ambient noise (Stehly et al. 2008; Ma and Beroza 2012; Sheng et al. 2018). This implementation is largely inspired by earthquake coda interferometry that utilizes scattered wave energy containing coherent information about the elastic response of Earth (Campillo and Paul 2003). An underlying assumption of the C^3 approach is that the long-term average of C^1 leads to the emergence of stable, predominantly time-invariant coda waves (Ma and Beroza 2012), thus enabling the reconstruction of GF between asynchronous stations using coda waves acquired at different times. Recent study has successfully applied C^3 to improve the resolution of crustal imaging in North America (Spica et al. 2017).

The ambient noise and coda waves are both diffuse wavefields that contain the energy from more homogeneously distributed sources surrounding the receivers. On the other hand, the usage of deterministic signals (e.g., surface waves from an earthquake or virtual sources) in GF retrieval is limited partially due to its biased spatial distribution and non-impulsive source time function. In this study, we examine the feasibility of constructing empirical GF from the deterministic wavefield. Specifically, we show that the cross-correlation of cross-correlation functions (hereafter C^2) from only a few virtual source stations within the stationary phase zone is sufficient to extract reliable GF. We demonstrate the effectiveness of the C^2 technique using the data collected from ALFREX network deployed in SW Australia (Figure 1), where GF is robustly reconstructed between asynchronous stations.

METHOD AND RESULTS

The process of GF retrieval is mathematically expressed as

$$G(x_B, x_A, t) \simeq u(x_B, t) \otimes u(x_A, t), \quad (1)$$

where $G(x_B, x_A, t)$ is the GF between receivers at locations x_A and x_B, and $u(x_A, t)$ and $u(x_B, t)$ are the corresponding seismic recordings and symbol $\otimes$ represents the cross-correlation operation. Equation (1) does not impose any constraints on the type of response recorded by the receiver, yet ambient noise imaging usually utilizes the stochastic signal (e.g., noise) and remove the contaminating deterministic signal (e.g., earthquakes) before cross-correlation (Bensen et al. 2007). We show later that such an implicit assumption is not always ideal for extracting GF using higher-order cross-correlation.

We first utilize standard noise correlation approach (i.e., C^1) for GF retrieval. We cut the continuous seismic recordings at each station into one hour segment. After removing the mean and linear trend, we downsample the data to 5 Hz and apply bandpass filtering between 150 and 0.5 sec to enhance the energy within the frequency band of interest. The processed (synchronous) time series from two stations are then cross-correlated and stacked to obtain the final C^1. Figure 2a shows clear surface wave energy emerged from C^1 that propagates across the elements of the array.

The process of GF retrieval from higher-order cross-correlation is formulated in the time domain as

$$G(x_B, x_A, t) \simeq \frac{1}{N}\sum_{i=1}^{N} G(x_B, S_i, t) \otimes G(x_A, S_i, t), \qquad (2)$$

where $G(x_A, S_i, t)$ and $G(x_B, S_i, t)$ are the empirical GFs approximated by C^1 between a temporary station at location x_A or x_B and a virtual source station at location S_i, and the summation of cross-correlation functions over N stations gives $G(x_B, x_A, t)$, the GF between x_A and x_B. Typically, the virtual source station is one of permanent stations from the backbone seismic network (e.g., Australian National Seismograph Network in our study; see inset in Figure 1). This representation is similar to source-receiver interferometry (Curtis et al. 2012; Curtis and Halliday 2010) but replacing the actual earthquake response with that from a virtual source located at x_A or x_B. It is worth noting that the two temporary stations need not to be operating at the same time so long as GFs from a common virtual source exist. Therefore, equation (2) provides a framework for reconstructing GF between asynchronous stations.

ALFREX network provides an ideal data set to test the proposed higher-order cross-correlation scheme (C^2). This network consists of two subarrays from two distinctive periods of acquisition, each sampling a part of the survey area (see Figure 1). There are also 13 semi-permanent stations operating throughout the whole deployment period, which serve as virtual source stations. To further increase the source coverage, we incorporate all available permanent stations across the Australian continent (see Figure 1).

The C^2 method we proposed exploits the information carried by the GF, which is different from C^3 that only utilizes the coda waves of C^1. We compare the performance of the two schemes in retrieving the GF among ALFREX stations, especially those operated asynchronously. To compute C^3, we perform cross-correlation over a 1200-sec long coda window that starts two times Rayleigh wave arrival following Stehly et al. (2008). The resulting C^3 exhibits prominent surface waves propagating between synchronous station pairs whereas no observable energy is extracted from asynchronous recordings (Figure 2b). In comparison, the GF obtained from C^2 produces clear surface wave energy with comparable quality in both cases (Figure 2c).

To evaluate the accuracy of the proposed method, we compute C^2 between synchronous station pairs where inter-station GF can be directly estimated from ambient noise field (i.e., C^1). We show a sample measurement between stations FB07 and FB08 located in the centre of the array to ensure good azimuthal coverage of the virtual sources. We compute the correlation coefficient of C^2 from each virtual source with C1 as a function of distance and azimuth (Figure 3a). The distribution of correlation coefficient shows a strong dependence on azimuth: high values are observed in the direction of azimuth and back-azimuth of the selected station pair and low values in the perpendicular direction. This observation is consistent with the stationary phase zone formalism (Snieder 2004) stating that only seismic sources distributed in the stationary phase zone contribute to the correct arrival times hence constructive stacking of seismic phases. The dependency of correlation coefficient on distance is weak, and factors such as site condition, local structures and ambient noise sources distributions may be responsible (see Figure 3a).

The stacked C^2 using virtual sources fall within the stationary phase zone, which is defined by a 45-degree azimuthal bin centred on the azimuth or back-azimuth directions of station pair, is highly consistent with the corresponding C^1 with a correlation coefficient of 0.86 (Figure 3b). Figure 3c shows each individual C^2 from 82 contributing sources, where Rayleigh type surface wave energy is clearly observable on either causal or acausal time axis, depending on the direction of the source.

As demonstrated in our experiment, one major advantage of C^2 over the C^3 method is its stability in GF retrieval. In the case of C^3, the cross-correlation of coda waves fails to extract any consistent phase arrivals between asynchronous stations, which is potentially attributed to a lack of coherent scattered wave energy from the far field stations or a biased spatial/temporal distribution of scattering sources. On the other hand, C^2 mostly relies on the deterministic energy from surface waves that are highly consistent over time, showing minimal changes after 3 months of stacking. Therefore, both synchronous and asynchronous stations exhibit a satisfactory recovery of GF.

The successful application of C^2 method only requires relatively short recording time, which is ideal for temporary networks such as ALFREX examined in our study. We show improvement in path coverage by incorporating asynchronous stations (Figure 4). This introduces 729 new ray paths that connecting the northernmost and southernmost parts of the array, which provides critical constraints to the long-wavelength structures underlying the network. Future studies will be focusing on applying seismic tomography using dispersion measurements from both C^1 and C^2 data sets. Another promising application of C^2 is its ability to tie temporary arrays deployed at different times (e.g., the campaign mode arrays in eastern Australia) to constrain the inter-array structure, which remains largely undersampled due to the current network topology. With much improved data sampling, the existing regional (e.g., Sippl et al. 2017) or continental scale crustal models (e.g., Saygin and Kennett 2012) can be further refined and eventually lead to a better understanding of the Australian continent.

CONCLUSIONS

Our study provides a new approach (C^2) to extract interstation GF through cross-correlating the deterministic energy from a far field station (virtual source). This technique essentially extends the C^3 method to the more general framework of source-station interferometry. Despite its promising application, a known issue of C^2 technique is that the signal-to-noise ratio of GF retrieved is typically lower than that from ambient noise correlation, which may increase the uncertainty in the measurement of dispersion data. More efficient stacking method (i.e., phase weighted stacking; Schimmel and Paulssen 1997) may help alleviate this problem. Overall, our study provides a useful tool to extract new information from the old datasets and has great potential to improve the quality of seismic imaging of the Australian continent.

ACKNOWLEDGMENTS

We thank David Howard for assistance on ALFREX data. We thank Mehdi Tork Qashqai for helpful discussions.

REFERENCES

Bensen, G. D. et al. 2007. "Processing Seismic Ambient Noise Data to Obtain Reliable Broad-Band Surface Wave Dispersion Measurements." *Geophysical Journal International* 169(3):1239–60.

Campillo, Michel and Anne Paul. 2003. "Long-Range Correlations in the Diffuse Seismic Coda." *Science* 299(5606):547–49.

Curtis, Andrew et al. 2012. "The Benefit of Hindsight in Observational Science: Retrospective Seismological Observations." *Earth and Planetary Science Letters*.

Curtis, Andrew and David Halliday. 2010. "Source-Receiver Wave Field Interferometry." *Physical Review E - Statistical, Nonlinear, and Soft Matter Physics* 81(4).

Lobkis, Oleg I. and Richard L. Weaver. 2001. "On the Emergence of the Green's Function in the Correlations of a Diffuse Field." *The Journal of the Acoustical Society of America* 110(6):3011–17.

Ma, Shuo and Gregory C. Beroza. 2012. "Ambient-Field Green's Functions from Asynchronous Seismic Observations." *Geophysical Research Letters*.

Saygin, Erdinc and B. L. N. Kennett. 2012. "Crustal Structure of Australia from Ambient Seismic Noise Tomography." *Journal of Geophysical Research: Solid Earth* 117(1):1–15.

Schimmel, Martin and Hanneke Paulssen. 1997. "Noise Reduction and Detection of Weak, Coherent Signals through Phase-Weighted Stacks." *Geophysical Journal International*.
Sheng, Yixiao, Nori Nakata, and Gregory C. Beroza. 2018. "On the Nature of Higher-Order Ambient Seismic Field Correlations." *Journal of Geophysical Research: Solid Earth*.

Sippl, C., B. L. N. Kennett, H. Tkalčić, K. Gessner, and C. V. Spaggiari. 2017. "Crustal Surface Wave Velocity Structure of the East Albany-Fraser Orogen, Western Australia, from Ambient Noise Recordings." *Geophysical Journal International*.

Snieder, Roel. 2004. "Extracting the Green's Function from the Correlation of Coda Waves: A Derivation Based on Stationary Phase." *Physical Review E* 69(4):46610.

Snieder, Roel and Eric Larose. 2013. "Extracting Earth's Elastic Wave Response from Noise Measurements." *Annual Review of Earth and Planetary Sciences*.

Spica, Zack, Mathieu Perton, and Gregory C. Beroza. 2017. "Lateral Heterogeneity Imaged by Small-Aperture ScS Retrieval from the Ambient Seismic Field." *Geophysical Research Letters*.

Stehly, Laurent, Michel Campillo, Brnice Froment, and Richard L. Weaver. 2008. "Reconstructing Green's Function by Correlation of the Coda of the Correlation (C3) of Ambient Seismic Noise." *Journal of Geophysical Research: Solid Earth* 113(B11).

Wapenaar, Kees, Deyan Draganov, Roel Snieder, Xander Campman, and Arie Verdel. 2010. "Tutorial on Seismic Interferometry: Part 1 — Basic Principles and Applications." *Geophysics*.

Weaver, Richard L. and Oleg I. Lobkis. 2001. "Ultrasonics without a Source: Thermal Fluctuation Correlations at Mhz Frequencies." *Physical Review Letters*.

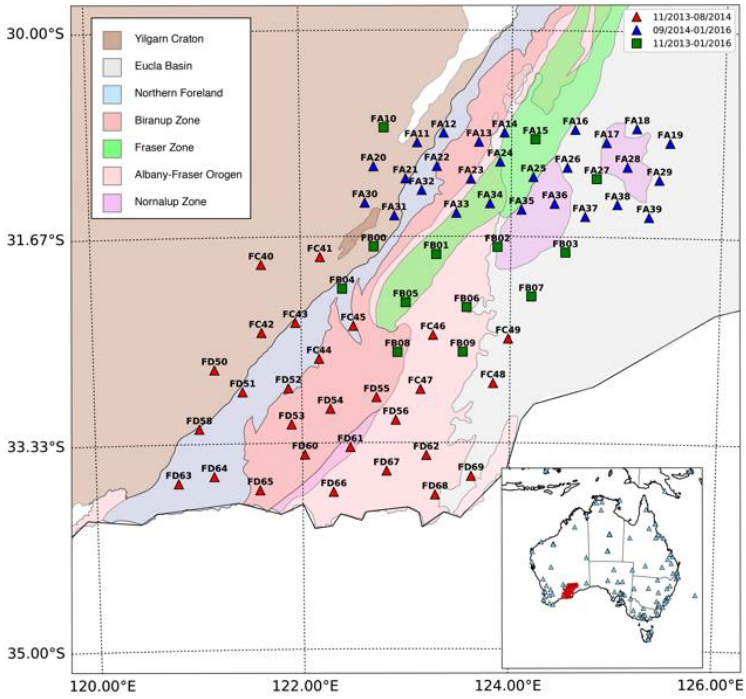

Figure 1. Spatio-temporal distribution of ALFREX network superimposed on a regional geological map of southwestern Australia. The inset shows the distribution of permanent stations (blue) acting as virtual sources in Green's function retrieval. The ALFREX network is highlighted in red.

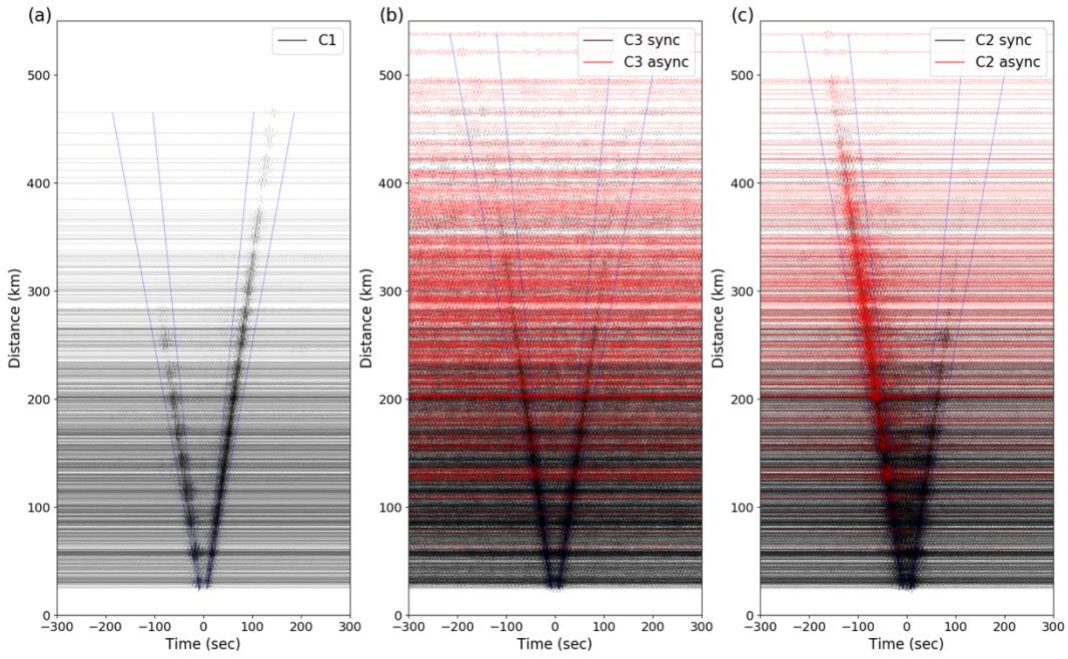

Figure 2. Green's function extracted from (a) C^1, (b) C^3 and (c) C^2 techniques for asynchronous and synchronous stations. The blue lines indicate the respective move-out velocities of 2.5 and 4.5 km/sec, indicating the excepted speed of surface wave propagation in the region of study.

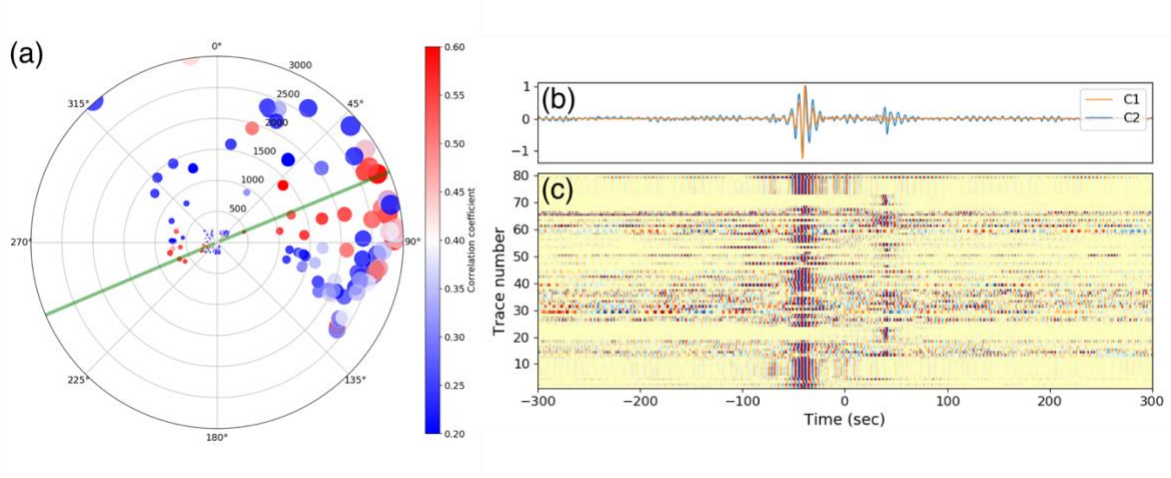

Figure 3. (a) Azimuthal and distance distribution of the correlation coefficient between C^1 and C^2. The green lines indicate the directions of azimuth and back-azimuth of the selected station pair. (b) Waveform comparison between C^1 (red) and stacked C^2 (blue) using virtual sources within the stationary phase zone. (c) Individual C^2 that contributes to the stacking in (b).

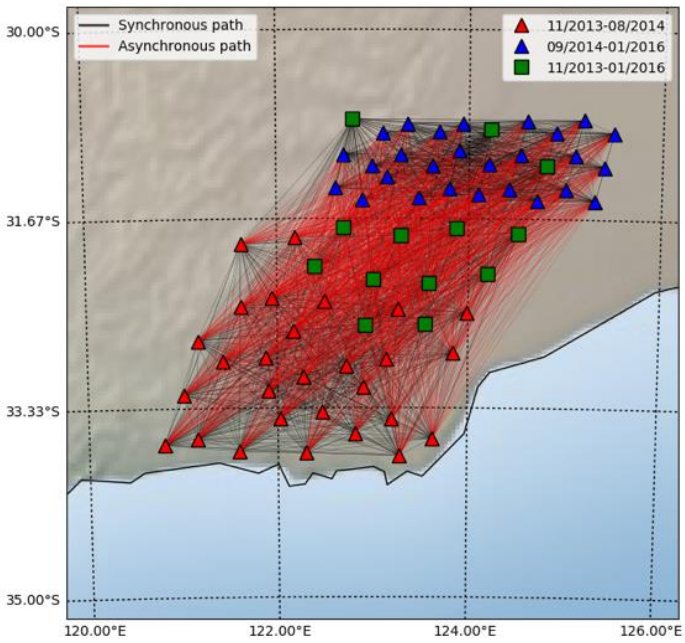

Figure 4. Seismic ray-path coverage from synchronous (black) and asynchronous (red) stations.